

Flat band effects on the ground-state BCS-BEC crossover in atomic Fermi gases in a quasi-two-dimensional Lieb lattice

Hao Deng,^{1,2,3} Chuping Li,^{1,2,3} Yuxuan Wu,^{1,2,3} Lin Sun,^{3,2,*} and Qijin Chen^{1,2,3,†}

¹*Hefei National Research Center for Physical Sciences at the Microscale and School of Physical Sciences, University of Science and Technology of China, Hefei, Anhui 230026, China*

²*Shanghai Research Center for Quantum Science and CAS Center for Excellence in Quantum Information and Quantum Physics, University of Science and Technology of China, Shanghai 201315, China*

³*Hefei National Laboratory, University of Science and Technology of China, Hefei 230088, China*

(Dated: October 20, 2023)

The ground-state superfluid behavior of ultracold atomic Fermi gases with an on-site attractive interaction in a quasi-two-dimensional Lieb lattice is studied using BCS mean-field theory, within the context of BCS-BEC crossover. We find that the flat band leads to nontrivial exotic effects. As the Fermi level enters the flat band, both the pairing gap and the in-plane superfluid density exhibit an unusual power law as a function of interaction, with strongly enhanced quantum geometric effects, in addition to a dramatic increase of compressibility as the interaction approaches the BCS limit. As the Fermi level crosses the van Hove singularities, the character of pairing changes from particle-like to hole-like or vice versa. We present the computed phase diagram, in which a pair density wave state emerges at high densities with relatively strong interaction strength.

Ultracold atomic Fermi gases in optical lattices have been of great interest over the past two decades, due to their multiple adjustable parameters, which renders them an ideal platform for quantum simulation and quantum engineering and thus have enormous potential for adding to our understanding of difficult condensed matter problems and exploring new quantum physics [1–5]. These adjustable parameters include interaction strength, lattice potential well depth, temperature, dimensionality, population imbalance, and lattice geometry, etc [6–10]. In particular, crossover from a BCS type of superfluidity to Bose–Einstein condensation (BEC) of fermion pairs in an attractive Hubbard model can be realized in an optical lattice using atomic Fermi gases in an optical lattice [11]. Such a BCS-BEC crossover has been realized by tuning the effective interaction strength through a Feshbach resonance in trapped atomic Fermi gases [12]. Such crossover studies can help to elucidate the underlying physics of the widespread pseudogap phenomenon in cuprate superconductors [13], which is of central importance in understanding the mechanism of high-temperature superconductivity [14].

Recently, models with a flat band have attracted great interest, because of the high density of states of the flat band and possible quantum geometric effect associated with multi-band of such systems. It has been reported that flat band and quantum geometric effect may enhance the superconducting transition temperature with an on-site attractive interaction and may give rise to quantum Hall states with a nonzero Chern number [15–20]. Flat bands have been studied in bipartite lattices, e.g., Lieb lattice, perovskite lattice, magic-angle graphene moiré lattices, as well as kagome and honeycomb lattices [15, 21–24].

Particularly, Lieb lattices have been realized in optical lattices of ultracold atoms [25, 26]. With line centers on a square, a Lieb lattice contains a central flat band, which touches an upper and a lower band at the Dirac points at the Brillouin zone

corners [27]. There have been a number of theoretical and experimental studies on Lieb lattices, including lattice preparation [25, 26, 28] and associated aspects including Chern semimetals with three spinless fermion species [29], ferromagnetic and antiferromagnetic states in a repulsive Hubbard model at half filling [30–32], strain-induced superconductor-insulator transition [33], and competition between pairing and charge density wave at half filling using determinant quantum Monte Carlo [34]. Moreover, quantum spin Hall effect has also been investigated in topological Lieb lattices, when the next-nearest-neighbor hopping associated with spin-orbit-coupling [19, 35, 36] or a Dzyaloshinskii-Moriya term is introduced [37]. Due to the rich physics in the presence of a Lieb lattice, it is important to investigate the superfluidity and pairing phenomenon of ultracold Fermi gases in a Lieb lattice, in order to uncover possible exotic and interesting new quantum phenomena in an attractive Hubbard model in the presence of a flat band.

In this Letter, we investigate the flat band effects on the ground-state superfluid behaviors of ultracold atomic Fermi gases in a quasi-two-dimensional Lieb lattice within a simple attractive Hubbard model, with the nearest neighbor hopping only, which leads to a zero Chern number for the flat band [38]. Among the three bands, we find that the flat band, as well as the van Hove singularities (VHS), strongly affects the superfluid behaviors, leading to many exotic phenomena. When the Fermi level enters the flat band, the fermion pairing gap changes from an exponential dependence into an unusual power law, as a function of the interaction strength, with an enormous compressibility κ in the BCS limit. At the same time, the superfluid density also exhibits a power law behavior, in contrast to being a constant in 3D free space. For a lower number density slightly above 1 fermion per unit cell, the fermion chemical potential μ exhibits a *nonmonotonic* behavior as a function of the interaction strength in the weak interaction region, and reaches a maximum when it crosses the VHS in the lower band, which signals a change of character of the pairing from particle-like at strong interactions to hole-like at weak interactions. At the same time, the compressibility κ

* Corresponding author: lsun22@ustc.edu.cn

† Corresponding author: qjc@ustc.edu.cn

is raised up in the weak coupling region as the Fermi level gets closer to the VHS in the lower band. Furthermore, in the BEC regime, μ asymptotically shows a linear dependence on the interaction strength $|g|$, leading to a density-independent $\kappa = -2/g$, with the pairing gap $\Delta \sim |\mu| \sim |g|$, which is qualitatively similar to the 3D lattice case [39]. Moreover, the ground-state phase diagram reveals that a pair density wave (PDW) ground state emerges at intermediate pairing strength for relatively large densities, as a consequence of strong inter-pair repulsive interactions and relatively large pair size at intermediate pairing strength, which is also found in dipolar Fermi gases [40] and Fermi gases in 2D optical lattice with 1D continuum dimension [41, 42] within the pairing fluctuation theory.

The Hamiltonian of our attractive Hubbard model in a Lieb lattice is given by

$$H = \sum_{\mathbf{k}\sigma} \hat{c}_{\mathbf{k}\sigma}^\dagger \hat{H}_{\mathbf{k}} \hat{c}_{\mathbf{k}\sigma} + g \sum_{\mathbf{k}\mathbf{k}' \mathbf{q}} \hat{c}_{\mathbf{k}+\frac{\mathbf{q}}{2}\uparrow}^\dagger \hat{c}_{-\mathbf{k}+\frac{\mathbf{q}}{2}\downarrow}^\dagger \hat{c}_{-\mathbf{k}'+\frac{\mathbf{q}}{2}\downarrow} \hat{c}_{\mathbf{k}'+\frac{\mathbf{q}}{2}\uparrow},$$

where $g < 0$, and

$$\hat{H}_{\mathbf{k}} = \begin{bmatrix} d_k & a_k & b_k \\ a_k & d_k & 0 \\ b_k & 0 & d_k \end{bmatrix}$$

is the Hamiltonian in momentum space for free fermions. Here $a_k = 2t[1 - \cos(k_x/2)]$ and $b_k = 2t[1 - \cos(k_y/2)]$ represent the hopping in the x and y directions, respectively, and $d_k = 2t_z(1 - \cos k_z) - \mu$ the dispersion in the out-of-plane \hat{z} direction, with t and t_z being the in-plane and out-of-plane hopping integral, respectively. We take $t_z/t = 0.01$ for the quasi-two dimensionality, set the lattice constant $a = 1$, and take the bottom of the lower energy band as the zero point of μ . Diagonalizing $\hat{H}_{\mathbf{k}}$ leads to three bands with dispersions $\xi_{\mathbf{k}}^\alpha = \alpha\sqrt{2t}\sqrt{2 + \cos k_x + \cos k_y} + 2\sqrt{2}t + 2t_z(1 - \cos k_z) - \mu$, where $\alpha = \pm, 0$ denotes the upper, the lower and the flat band, respectively.

Using the BCS mean-field theory at zero temperature, the bare and full Green's functions are given by

$$G_0(K) = \frac{\theta(|k| - k_F)}{\omega - \hat{H}_{\mathbf{k}} + i0^+} + \frac{\theta(k_F - |k|)}{\omega - \hat{H}_{\mathbf{k}} - i0^+},$$

$$G^{-1}(K) = G_0^{-1}(K) - \Delta^2 \tilde{G}_0(K),$$

respectively, where $\tilde{G}_0(K) = -G_0^T(-K)$ with four momentum $K \equiv (\omega, \mathbf{k})$, and $\theta(x)$ is the Heaviside step function. Thus one has the self energy $\Sigma(K) = \Delta^2 \tilde{G}_0(K)$.

Under the number constraint $n = 2 \sum_K \text{Tr} G(K)$ with $\sum_K \equiv \sum_\omega \sum_{\mathbf{k}}$, we have the number equation

$$n = \sum_{\mathbf{k}} \sum_{\alpha=0,\pm} \left(1 - \frac{\xi_{\mathbf{k}}^\alpha}{E_{\mathbf{k}}^\alpha} \right), \quad (1)$$

where $E_{\mathbf{k}}^\alpha = \sqrt{(\xi_{\mathbf{k}}^\alpha)^2 + \Delta^2}$ is the Bogoliubov quasiparticle dispersion for the $\alpha = \pm, 0$ band with an energy gap Δ . And the gap equation is given by

$$0 = \frac{1}{g} + \sum_{\mathbf{k}} \sum_{\alpha=0,\pm} \frac{1}{2E_{\mathbf{k}}^\alpha}. \quad (2)$$

Equations (1) and (2) form a closed set of self-consistent equations, which can be solved for (μ, Δ) as a function of g in the superfluid phase.

Furthermore, the solution for (μ, Δ) from Eqs.(1) and (2) should satisfy the stability condition for the superfluid phase that the energy spectrum of Cooper pairs should be non-negative. To this end, we extract the pair dispersion using the fluctuating pair propagator, as given in the pairing fluctuation theory which was previously developed for the pseudogap physics in the cuprates [14], and has been extended to address the BCS-BEC crossover in ultracold atomic Fermi gases [1]. To be compatible [43] with the BCS-Leggett ground state, the pairing susceptibility in the T -matrix $t_{\text{pg}}^{-1}(Q) = 1/g + \chi(Q)$ is given by $\chi(Q) = -\sum_K \text{Tr}[G(K)\tilde{G}_0(K - Q)]$, with $Q \equiv (\Omega, \mathbf{q})$, which leads to $t_{\text{pg}}^{-1}(\Omega, \mathbf{q}) \approx a_0(\Omega - \Omega_{\mathbf{q}})$ in the superfluid phase, with the pair dispersion $\Omega_{\mathbf{q}} = 2B(2 - \cos q_x - \cos q_y) + 2B_z(1 - \cos q_z)$. Here B and B_z correspond to the effective pair hopping integral in the xy plane and in the z direction, respectively. The expressions for the coefficients a_0 , B and B_z can be readily derived during the Taylor expansion. The non-negativeness of the pair dispersion requires that the pairing correlation length (squared) $\xi^2 = a_0 B$ and $\xi_z^2 = a_0 B_z$ be positive.

Superfluid density is an important transport property, which is correlated with condensed pairs; its dependence on the interaction strength often reflects the pairing symmetry. It takes the average of the inverse band mass in the presence of a lattice, in contrast with the 3D continuum case where it is always given by n/m at zero T in BCS theory. Moreover, the in-plane component of the superfluid density can be divided into a conventional and a geometric part, due to the existence of the flat band, where the geometric term is associated with the interband matrix elements of the current operator, which is proportional to a quantum metric tensor.

The in-plane superfluid density $(n_s/m)_{\parallel}$ contains a conventional term $(n_s/m)_{\parallel}^{\text{conv}}$ and a geometric term $(n_s/m)_{\parallel}^{\text{geom}}$, i.e., [44]

$$\left(\frac{n_s}{m} \right)_{\parallel} = \left(\frac{n_s}{m} \right)_{\parallel}^{\text{conv}} + \left(\frac{n_s}{m} \right)_{\parallel}^{\text{geom}}, \quad (3)$$

where

$$\left(\frac{n_s}{m} \right)_{\parallel}^{\text{conv}} = \frac{t^2}{4} \sum_{\mathbf{k}} \sum_{\alpha=\pm} \frac{\Delta^2}{(E_{\mathbf{k}}^\alpha)^3} \frac{\sin^2 k_x + \sin^2 k_y}{2 + \cos k_x + \cos k_y}, \quad (4)$$

$$\left(\frac{n_s}{m} \right)_{\parallel}^{\text{geom}} = \Delta^2 \sum_{\mathbf{k}} \left[\left(\frac{1}{E_{\mathbf{k}}^+} - \frac{1}{E_{\mathbf{k}}^-} \right) \frac{\xi_{\mathbf{k}} - \xi_{\mathbf{k}}^+}{\xi_{\mathbf{k}} + \xi_{\mathbf{k}}^+} + \left(\frac{1}{E_{\mathbf{k}}^-} - \frac{1}{E_{\mathbf{k}}^+} \right) \frac{\xi_{\mathbf{k}} - \xi_{\mathbf{k}}^-}{\xi_{\mathbf{k}} + \xi_{\mathbf{k}}^-} \right] (g_{xx} + g_{yy}). \quad (5)$$

Here $g_{\mu\nu} = \text{Re}(\partial_\mu \langle + |)(1 - |+ \rangle \langle + |)\partial_\nu |+\rangle$ is the quantum metric tensor of the upper or the lower band, where $|\pm\rangle$ is the eigenvector of $H_{\mathbf{k}}$, associated with the upper and lower free bands, respectively. The out-of-plane component reads

$$\left(\frac{n_s}{m} \right)_z = 2t_z^2 \sum_{\mathbf{k}} \sum_{\alpha=\pm} \frac{\Delta^2}{(E_{\mathbf{k}}^\alpha)^3} \sin^2 k_z. \quad (6)$$

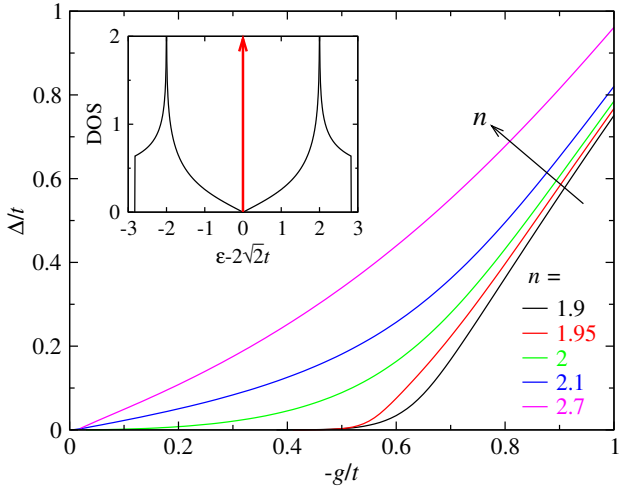


Figure 1. Δ as a function of $-g$ for various n in the weak coupling BCS regime, with μ close to or inside the flat band. Shown in the inset is the DOS for strict 2D case, where the (red) arrow denotes the flat band.

Compressibility κ is one of the most important physical quantities in thermodynamic physics, which must be positive to maintain mechanical stability. For the ground-state compressibility [45], one has

$$\begin{aligned} \kappa &= \frac{\partial n}{\partial \mu} = \left(\frac{\partial n}{\partial \mu} \right)_\Delta + \left(\frac{\partial n}{\partial \Delta} \right)_\mu \frac{\partial \Delta}{\partial \mu} \\ &= \sum_{k\alpha} \frac{\Delta^2}{(E_k^\alpha)^3} + \frac{\left[\sum_{k\alpha} \xi_k^\alpha / (E_k^\alpha)^3 \right]^2}{\sum_{k\alpha} 1 / (E_k^\alpha)^3}. \end{aligned} \quad (7)$$

One can tell that κ reflects the property of density of state (DOS). In the weak coupling regime, a larger DOS at the Fermi level corresponds to a higher κ . Especially, κ reduces to the DOS in the noninteracting limit.

The asymptotic behavior in the BEC limit can be solved analytically with $\mu \rightarrow -\infty$. The gap and number equations yield

$$\mu = \frac{(3-n)g}{2} + 2\sqrt{2}t, \quad (8)$$

$$\Delta = \sqrt{\frac{9}{4}g^2 - \mu^2}, \quad (9)$$

respectively, with a scaling behavior qualitatively similar to $\Delta \sim |\mu| \sim |g|$ for 3D lattice. Thus, we obtain for all densities the BEC asymptote

$$\kappa = -\frac{2}{g}. \quad (10)$$

We first investigate the flat band effects on the pairing gap behavior, when the Fermi level is close to or within the flat band. Due to the particle-hole symmetry, we restrict $n \leq 3$, and the Fermi level enters the flat band for $n \geq 2$ in the noninteracting limit. Plotted in Fig. 1 is Δ versus $-g$ (in units of t) for various densities near $n \lesssim 2$ and $n \in [2, 3]$ in the weak coupling BCS regime. Shown in the inset is the DOS

for the strict 2D case, where the (red) vertical arrow denotes the flat band, along with two VHS's in the upper and lower bands, corresponding to $n = 1$ and 5 , respectively. For $n < 2$, including $n = 1.95$, Δ exhibits an exponentially activated behavior in the weak coupling regime, similar to its counterpart in 3D continuum and 3D cubic lattices. This is expected in BCS theory, under the approximation of a constant DOS near the Fermi surface. However, as the density goes higher than $n = 2$, the Fermi level enters the flat band with the lower band fully filled, and the behavior of Δ changes into an unusual power law, which can be attributed to the breakdown of the constant DOS approximation. Similar behavior has also been predicted within the dynamical mean-field theory in a quasi 2D *repulsive* Lieb lattice, where the magnetism as a function of the interaction changes from exponential to power law behavior at half filling [31]. The behavior of Δ over a broad range is shown in the inset of Fig. 2(b) on a log-log scale for a lower density, $n = 0.6$, which shows that the numerical result (black solid line) approaches its analytical BEC asymptote (red dashed line) in the deep BEC regime, as given by Eq. (9).

This unusual power-law behavior of Δ versus g can be explained following Ref. [31], despite the different signs of the interaction. Using the normalized, dimensionless notation $\bar{X} \equiv X/W$, where $W = 4\sqrt{2}t + 4t_z$ is the bandwidth, the rescaled, dimensionless DOS can be approximated as $\bar{\rho}(\bar{\varepsilon}) \equiv W\rho(\bar{\varepsilon}) = 4\theta(1/2 - |\bar{\varepsilon} - 1/2|) + 2\delta(\bar{\varepsilon} - 1/2)$, where the δ function represents the flat band.

For $n > 2$, using this $\bar{\rho}(\bar{\varepsilon})$ for the integral in the gap equation (2), we obtain

$$\bar{\Delta} = \frac{n-2}{4\mathcal{W}(\frac{n-2}{4}\exp(\frac{1}{2|\bar{g}|}))},$$

where \mathcal{W} is the Lambert \mathcal{W} -function, which is the inverse function of $f(\mathcal{W}) = \mathcal{W}\exp(\mathcal{W})$. For small $x \rightarrow 0$, $\mathcal{W}(x) \approx x - x^2 + 3x^3/2$. This leads to $\bar{\Delta} \propto (n-2)|\bar{g}|$ for $n > 2$ in the weak coupling regime. At low $n < 2$, the δ -function term in $\bar{\rho}(\bar{\varepsilon})$ becomes irrelevant, so that we recover the ordinary BCS behavior, $\bar{\Delta} \propto \exp(1/n\bar{g})$.

Next, we show in Fig. 2 the behaviors of μ as a function of $-g$ for various n , so that the Fermi level changes from (a) the lower band below ($n = 0.6$) and around the VHS ($0.9 \leq n \leq 1.2$) to (b) near ($n = 1.9, 1.95$) or inside the flat band ($n = 2, 2.3, 2.7$). As shown in the inset of Fig. 2(a), $-\mu$ (black solid line, for $n = 0.6$) approaches its BEC asymptotic behavior (red dashed line) for $-g/t > 10$. For $n \leq 1$ in Fig. 2(a), μ decreases monotonically as the pairing interaction becomes stronger, similar to that in a regular one-band model below half filling. However, for $n = 1.1, 1.2$, μ exhibits a remarkable nonmonotonic behavior in the weak coupling BCS regime; μ increases first as the pairing becomes stronger, and then starts to decrease after passing a maximum. Such nonmonotonicity is also found in a 2D optical lattice with a strong lattice effect, which is comprised of two lattice and one continuum dimensions [41, 42]. In a quasi-2D Lieb lattice, the lower band has two VHS's, at $\varepsilon = (2\sqrt{2} - 2)t \approx 0.8284t$ and $\varepsilon = (2\sqrt{2} - 2)t + 4t_z \approx 0.8684t$. For $n = 1.1, 1.2$, $\mu > 0.8684t$ for small $|g|$, i.e., the Fermi level sits slightly

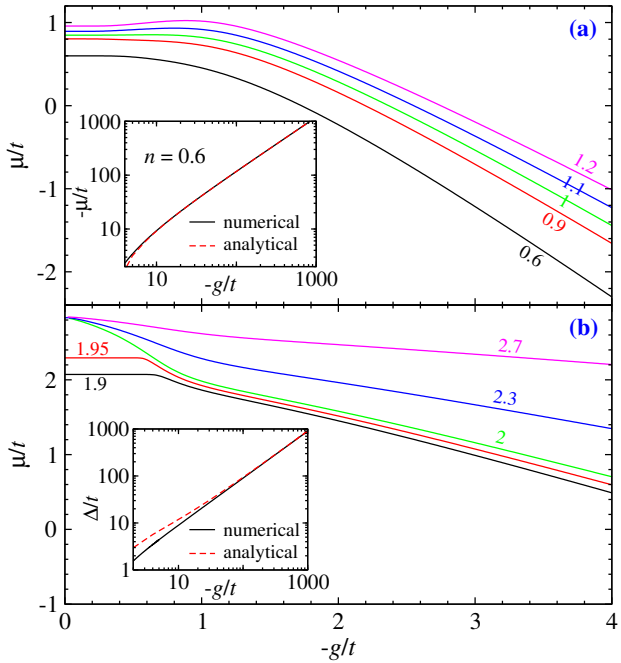


Figure 2. Evolution of μ as a function of $-g/t$ for small $0.6 \leq n \leq 1.2$ in panel (a) and large $1.9 \leq n \leq 2.7$ in panel (b), as labeled. Shown in the insets of panels (a) and (b) is a comparison between the full numerical solution (black solid) and the analytical BEC asymptotic behavior (red dashed) of $-\mu$ and Δ , respectively, as a function of $-g/t$ on a log-log scale for $n = 0.6$.

above the VHS's, where the DOS $\rho(\varepsilon)$ has a negative slope, so that the pairing becomes hole-like, for which μ increases as the pairing becomes stronger, as in a 3D cubic lattice above half filling. As pairing strength increases further, the contribution of the DOS below the VHS's comes in, so that μ starts to decrease again. As n increases and approaches $n = 2$, the flat band gradually affects the behaviors of μ in the BCS regime. For $n = 1.9, 1.95$ in Fig. 2(b), μ remains nearly a constant before decreasing as $-g$ increases in the BCS regime. For $2 \leq n \leq 3$, μ enters the flat band, and starts to decrease from roughly the same noninteracting limit $\mu_0 \approx 2\sqrt{2}t$. While the nearly constant μ for $n = 1.9, 1.95$ is in accord with the exponentially small gap in the BCS regime (Fig. 1), a power-law decrease in μ can be readily seen for $n \in [2, 3]$, commensurate with the power-law increase of Δ as a function of $-g$.

Shown in Fig. 3 are the in-plane (left column) and out-of-plane (right column) superfluid density, from top to bottom, for $n = 0.6, 2$ and 2.7 , respectively, as well as the conventional $(n_s/m)_{\parallel}^{\text{conv}}$ (blue) and geometric part $(n_s/m)_{\parallel}^{\text{geom}}$ (red curves) of $(n_s/m)_{\parallel}$. For $n = 0.6$, both the in-plane $(n_s/m)_{\parallel}$ and out-of-plane $(n_s/m)_z$, as well as the conventional $(n_s/m)_{\parallel}^{\text{conv}}$, exhibit a roughly constant behavior as a function of $-g$ in the weak coupling regime, similar to the constant superfluid density n/m in 3D free space. On the contrary, the geometric part $(n_s/m)_{\parallel}^{\text{geom}}$ vanishes in the noninteracting limit. Commensurate with the evolution of Δ versus $-g$, as n increases to $n \geq 2$, the behaviors of both $(n_s/m)_{\parallel}^{\text{conv}}$

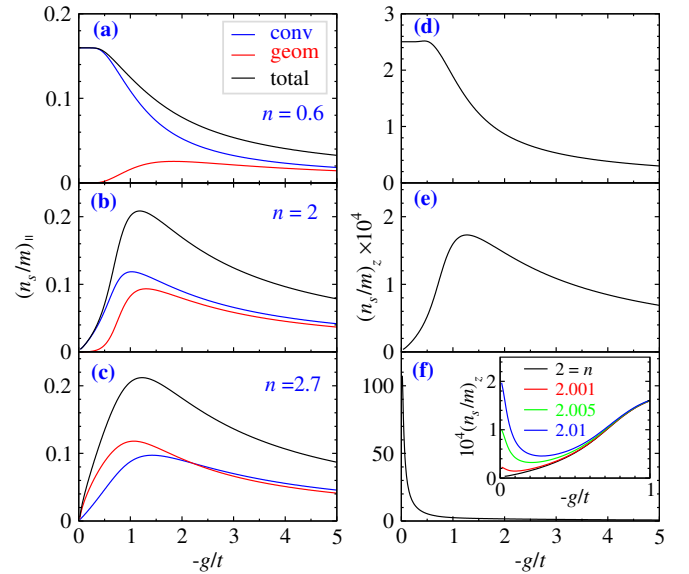


Figure 3. Behavior of the in-plane superfluid density $(n_s/m)_{\parallel}$ (black curves) along with its conventional (blue curves) and geometric parts (red curves), as a function of $-g/t$, for (a) $n = 0.6$, (b) 2 , (c) 2.7 . Plotted in (d-f) are the corresponding out-of-plane superfluid density $(n_s/m)_z$. Shown in the inset of panel (f) is $(n_s/m)_z$ in the weak interaction regime for a series of $n \gtrsim 2$.

and $(n_s/m)_{\parallel}^{\text{geom}}$, as well as $(n_s/m)_{\parallel}$, evolve into power laws as a function of $-g$. More importantly, $(n_s/m)_{\parallel}^{\text{conv}}$ now approaches zero in the noninteracting limit, unlike in a simple cubic lattice. This can be attributed to a few reasons. (i) Without the out-of-plane contribution, the DOS from the upper and lower band is zero when μ falls inside the flat band. (ii) There is a perfect particle-hole symmetry at this μ so that the contributions from particles and holes cancel out in $(n_s/m)_{\parallel}$. (iii) The quantum geometric contribution relies on a finite gap Δ , and hence vanishes in the zero g limit. (iv) The flat band does not contribute to superfluidity without the quantum geometric effect. As μ moves away from the flat band with increasing $|g|$, the particle-hole cancellation breaks down, leading to a rising $(n_s/m)_{\parallel}$. As $|g|$ increases further toward the BEC regime, $(n_s/m)_{\parallel}$ starts to decrease due to the lattice effects. Without a geometric contribution, the out-of-plane superfluid density $(n_s/m)_z$ exhibits a behavior similar to that of $(n_s/m)_{\parallel}^{\text{conv}}$ in the weak coupling regime for $n = 0.6$ and 2 . However, difference appears as μ enters the flat band. As shown in the inset of Fig. 3(f), when n becomes slightly higher than 2 , $(n_s/m)_z$ starts to increase as the noninteracting limit is approached. At $n = 2.7$, shown in Fig. 3(f), this increase is so dramatic that $(n_s/m)_z$ becomes monotonically decreasing with $|g|$. This distinct behavior of $(n_s/m)_z$, compared to $(n_s/m)_{\parallel}^{\text{conv}}$, results from the broadening of the flat band due to the small out-of-plane dispersion with $t_z/t = 0.01$.

We now plot in Fig. 4 the compressibility κ versus $-g$ for (a) small n below and around the VHS and (b) large n near the flat band bottom. Figure 4(a) indicates that the noninteracting value of κ reaches a local maximum at the VHS

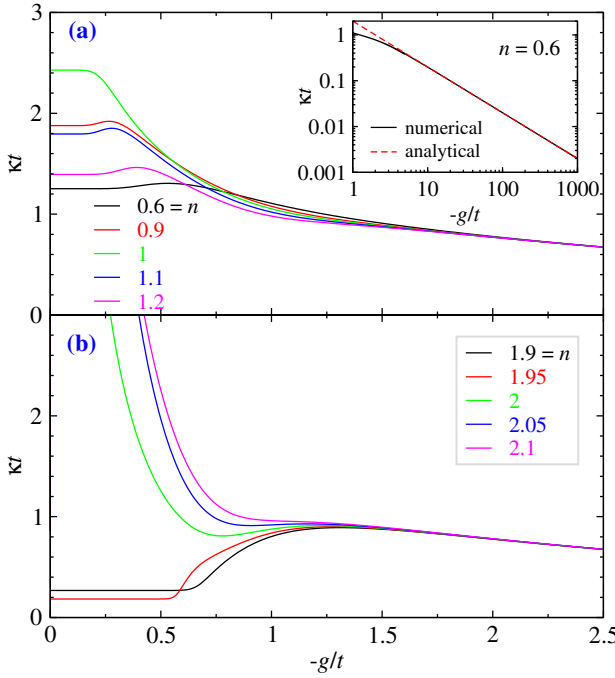


Figure 4. κ versus $-g$ for (a) small n below ($n = 0.6$) and close to the van Hove singularities around $n = 1$ and (b) large n near the bottom of the flat band $n = 2$. Shown in the inset of panel (a) is the comparison between the full numerical solution (black solid) and the analytical BEC asymptotic behavior (red dashed) of κ as a function of $-g$ on a log-log scale for $n = 0.6$.

$n = 1$ as a function of n , since this value is given by the DOS. Furthermore, for $n \in [0.9, 1.2]$, κ exhibits a nonmonotonic dependence on $|g|$, which is largely related to the non-monotonic behavior of $\mu(g)$. As the interaction goes stronger into the BEC regime, all fermions pair up and the two-body binding energy of the fermions dominates μ . As a consequence, κ decreases and approaches the same n -independent BEC asymptote. Indeed, as shown in the inset for $n = 0.6$, κ approaches nicely its analytical n -independent BEC asymptote when $-g/t > 10$. The nearly constant κ for $n = 1.9$ and 1.95 in Fig. 4(b) is clearly associated with the constant behavior of μ in the BCS regime shown in Fig. 2(b). For $n \geq 2$, κ increases sharply as the interaction strength decreases toward zero. Here the Fermi level falls within the flat band, and thus senses a huge DOS, which is equal to the noninteracting κ . Therefore, there is a jump of $\kappa(g=0)$ as n crosses the $n = 2$ boundary, as shown in Fig. 4(b).

Finally, we present in Fig. 5 the ground-state phase diagram in the $n - g$ plane. Here the positivity of $\xi^2 = a_0 B$ and $\xi_z^2 = a_0 B_z^2$ constitutes two stability conditions for the superfluid phase. The (black dot-dashed) $\mu = 0$ curve separates the fermionic superfluid regime on the upper left from the bosonic superfluid regime on the lower right. A PDW ground state with negative $\xi^2 < 0$ and/or $\xi_z^2 < 0$ emerges in the grey shaded region, enclosed inside the red $B = 0$ curve and blue $B_z = 0$ curve. Note that the upper branch of $B = 0$ overlaps nearly precisely with $B_z = 0$, and both are close to but falls slightly inside the fermionic side of the $\mu = 0$ line. The PDW

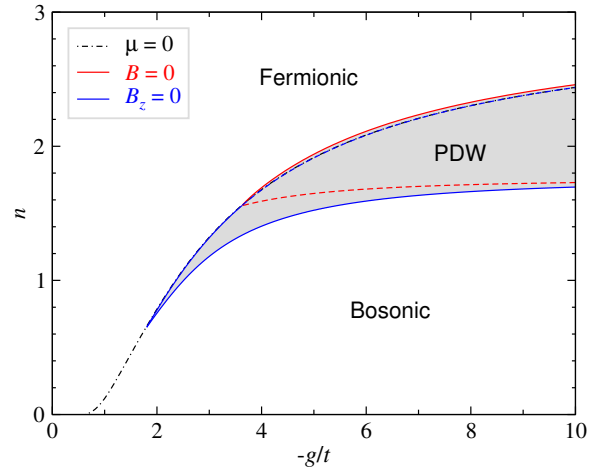


Figure 5. The ground-state phase diagram in the $n - g$ plane. The black dot-dashed $\mu = 0$ curve divides the plane into fermionic and bosonic superfluid regimes. Enclosed within the (red) $B = 0$ and (blue) $B_z = 0$ lines is a PDW ground state (gray shaded region).

state at intermediate and strong coupling for relatively large n is associated with the strong repulsive inter-pair interaction U and relatively low kinetic energy of the pairs, T , which leads naturally to Wigner crystallization. Indeed, for N pairs, the inter-pair interaction energy E_P scales as $N^2 U/2$ whereas the kinetic energy E_K scales as NT , allowing $E_P > E_K$ with a large U and lattice suppressed T . Technically, the sign of ξ^2 (or ξ_z^2) becomes negative between the $B = 0$ (or $B_z = 0$) curve, indicating that the minimum of the pair dispersion $\tilde{\Omega}_{\mathbf{q}}$ has moved from $\mathbf{q} = 0$ to a finite \mathbf{q} , with the crystallization wave vector in the xy plane (or in the z direction). The PDW state has been observed in experiments [46], but it is still unclear whether it can sustain superfluidity and thus becomes a supersolid, which will be left to a future study. Similar PDW ground state has been found in 3D optical lattice at high density [39], 2D optical lattice with strong lattice effect [41, 42], optical lattice in mixed dimensions [47], and in dipolar Fermi gases [40].

In summary, we have studied the ground-state superfluid properties of ultracold Fermi gases in a quasi-2D Lieb lattice in the context of BCS-BEC crossover, whose BEC asymptotic solution can be derived analytically. We find that the flat band, together with the van Hove singularities, have an extraordinary effect on the superfluid behaviors. When the Fermi level falls within the flat band, the pairing gap and the in-plane superfluid density exhibit an unusual power law in the weak coupling regime as a function of the interaction strength. Meanwhile, the compressibility increases sharply in the non-interacting limit. As the chemical potential increases across the VHS's in the lower band, the pairing becomes hole-like for weak interactions, leading to a nonmonotonic behavior of the chemical potential as a function of interaction strength. A PDW ground state emerges for intermediate and strong pairing strength with relatively large density. These findings for the Lieb lattice are very different from that for pure 3D continua and 3D cubic lattices and should be tested in future ex-

periments.

This work was supported by the Innovation Pro-

gram for Quantum Science and Technology (Grant No. 2021ZD0301904).

[1] Q. J. Chen, J. Stajic, S. N. Tan, and K. Levin, BCS–BEC crossover: From high temperature superconductors to ultracold superfluids, *Phys. Rep.* **412**, 1 (2005).

[2] I. Bloch, J. Dalibard, and W. Zwerger, Many-body physics with ultracold gases, *Rev. Mod. Phys.* **80**, 885 (2008).

[3] W. Zwerger, *The BCS-BEC crossover and the unitary Fermi gas*, Vol. 836 (Springer Science & Business Media, 2011).

[4] R. A. Hart, P. M. Duarte, T.-L. Yang, X. Liu, T. Paiva, E. Khatami, R. T. Scalettar, N. Trivedi, D. A. Huse, and R. G. Hulet, Observation of antiferromagnetic correlations in the Hubbard model with ultracold atoms, *Nature* **519**, 211+ (2015).

[5] I. Bloch, Quantum coherence and entanglement with ultracold atoms in optical lattices, *Nature* **453**, 1016 (2008).

[6] B. DeMarco and D. S. Jin, Onset of Fermi Degeneracy in a Trapped Atomic Gas, *Science* **285**, 1703 (1999).

[7] M. Bartenstein, A. Altmeyer, S. Riedl, S. Jochim, C. Chin, J. H. Denschlag, and R. Grimm, Crossover from a molecular Bose-Einstein condensate to a degenerate Fermi gas, *Phys. Rev. Lett.* **92**, 120401 (2004).

[8] J. Kinast, A. Turlapov, J. E. Thomas, Q. Chen, J. Stajic, and K. Levin, Heat capacity of a strongly interacting Fermi gas, *Science* **307**, 1296 (2005).

[9] M. Zwierlein, A. Schirotzek, C. Schunck, and W. Ketterle, Fermionic superfluidity with imbalanced spin populations, *Science* **311**, 492 (2006).

[10] G. Partridge, W. Li, R. Kamar, Y. Liao, and R. Hulet, Pairing and phase separation in a polarized Fermi gas, *Science* **311**, 503 (2006).

[11] D. Jaksch, C. Bruder, J. I. Cirac, C. W. Gardiner, and P. Zoller, Cold bosonic atoms in optical lattices, *Phys. Rev. Lett.* **81**, 3108 (1998).

[12] C. Chin, R. Grimm, P. Julienne, and E. Tiesinga, Feshbach resonances in ultracold gases, *Rev. Mod. Phys.* **82**, 1225 (2010).

[13] T. Timusk and B. Statt, The pseudogap in high-temperature superconductors: an experimental survey, *Rep. Prog. Phys.* **62**, 61 (1999).

[14] Q. J. Chen, I. Kosztin, B. Jankó, and K. Levin, Pairing fluctuation theory of superconducting properties in underdoped to overdoped cuprates, *Phys. Rev. Lett.* **81**, 4708 (1998).

[15] Y. Cao, V. Fatemi, S. Fang, K. Watanabe, T. Taniguchi, E. Kaxiras, and P. Jarillo-Herrero, Unconventional superconductivity in magic-angle graphene superlattices, *Nature* **556**, 43 (2018).

[16] N. B. Kopnin, T. T. Heikkilä, and G. E. Volovik, High-temperature surface superconductivity in topological flat-band systems, *Phys. Rev. B* **83**, 220503(R) (2011).

[17] V. J. Kauppinen, F. Aikebaier, and T. T. Heikkilä, Flat-band superconductivity in strained Dirac materials, *Phys. Rev. B* **93**, 214505 (2016).

[18] Y.-F. Wang, Z.-C. Gu, C.-D. Gong, and D. N. Sheng, Fractional quantum hall effect of hard-core bosons in topological flat bands, *Phys. Rev. Lett.* **107**, 146803 (2011).

[19] W. Beugeling, J. C. Everts, and C. Morais Smith, Topological phase transitions driven by next-nearest-neighbor hopping in two-dimensional lattices, *Phys. Rev. B* **86**, 195129 (2012).

[20] Z. Q. Wang, G. Chaudhary, Q. J. Chen, and K. Levin, Quantum geometric contributions to the BKT transition: Beyond mean field theory, *Phys. Rev. B* **102**, 184504 (2020), arXiv:2007.15028.

[21] E. H. Lieb, Two theorems on the Hubbard model, *Phys. Rev. Lett.* **62**, 1201 (1989).

[22] K. Sun, Z. Gu, H. Katsura, and S. Das Sarma, Nearly flatbands with nontrivial topology, *Phys. Rev. Lett.* **106**, 236803 (2011).

[23] E. Tang, J.-W. Mei, and X.-G. Wen, High-temperature fractional quantum hall states, *Phys. Rev. Lett.* **106**, 236802 (2011).

[24] T. Neupert, L. Santos, C. Chamon, and C. Mudry, Fractional quantum hall states at zero magnetic field, *Phys. Rev. Lett.* **106**, 236804 (2011).

[25] S. Taie, H. Ozawa, T. Ichinose, T. Nishio, S. Nakajima, and Y. Takahashi, Coherent driving and freezing of bosonic matter wave in an optical Lieb lattice, *Sci. Adv.* **1**, 10.1126/sciadv.1500854 (2015).

[26] F. Schafer, T. Fukuhara, S. Sugawa, Y. Takasu, and Y. Takahashi, Tools for quantum simulation with ultracold atoms in optical lattices, *Nat. Rev. Phys.* **2**, 411 (2020).

[27] K.-E. Huhtinen, M. Tylutki, P. Kumar, T. I. Vanhala, S. Peotta, and P. Törmä, Spin-imbalanced pairing and Fermi surface deformation in flat bands, *Phys. Rev. B* **97**, 214503 (2018).

[28] B. Cui, X. Zheng, J. Wang, D. Liu, S. Xie, and B. Huang, Realization of Lieb lattice in covalent-organic frameworks with tunable topology and magnetism, *Nat. Commun.* **11**, 66 (2020).

[29] G. Palumbo and K. Meichanetzidis, Two-dimensional Chern semimetals on the Lieb lattice, *Phys. Rev. B* **92**, 235106 (2015).

[30] K. Noda, A. Koga, N. Kawakami, and T. Pruschke, Ferromagnetism of cold fermions loaded into a decorated square lattice, *Phys. Rev. A* **80**, 063622 (2009).

[31] K. Noda, K. Inaba, and M. Yamashita, Magnetism in the three-dimensional layered Lieb lattice: Enhanced transition temperature via flat-band and Van Hove singularities, *Phys. Rev. A* **91**, 063610 (2015).

[32] W. Nie, D. Zhang, and W. Zhang, Ferromagnetic ground state of the SU(3) Hubbard model on the Lieb lattice, *Phys. Rev. A* **96**, 053616 (2017).

[33] N. Swain and M. Karmakar, Strain-induced superconductor-insulator transition on a Lieb lattice, *Phys. Rev. Res.* **2**, 023136 (2020).

[34] V. I. Iglovikov, F. Hébert, B. Grémaud, G. G. Batrouni, and R. T. Scalettar, Superconducting transitions in flat-band systems, *Phys. Rev. B* **90**, 094506 (2014).

[35] W. Zhu, S. Hou, Y. Long, H. Chen, and J. Ren, Simulating quantum spin hall effect in the topological Lieb lattice of a linear circuit network, *Phys. Rev. B* **97**, 075310 (2018).

[36] E. Sadeghi and H. Rezania, Spin-orbit coupling effects on transport properties of electronic Lieb lattice in the presence of magnetic field, *Sci. Rep.* **12**, 10.1038/s41598-022-12588-5 (2022).

[37] A. Pires, Transport on the ferromagnetic Lieb lattice, *J. Magn. Magn. Mater.* **547**, 168941 (2022).

[38] L. Chen, T. Mazaheri, A. Seidel, and X. Tang, The impossibility of exactly flat non-trivial Chern bands in strictly local periodic tight binding models, *J. Phys. A: Math. Theor.* **47**, 152001 (2014).

[39] C.-C. Chien, Q. J. Chen, and K. Levin, Fermions with attractive interactions on optical lattices and implications for correlated systems, *Phys. Rev. A* **78**, 043612 (2008).

- [40] Y. M. Che, J. B. Wang, and Q. J. Chen, Reentrant superfluidity and pair density wave in single-component dipolar Fermi gases, *Phys. Rev. A* **93**, 063611 (2016).
- [41] L. Sun, J. B. Wang, X. Chu, and Q. J. Chen, Pairing phenomena and superfluidity of atomic Fermi gases in a two-dimensional optical lattice: Unusual effects of lattice-continuum mixing, *Annalen der Physik* **534**, 2100511 (2022).
- [42] L. Sun and Q. J. Chen, Ground states of atomic Fermi gases in a two-dimensional optical lattice with and without population imbalance, *Phys. Rev. A* **106**, 013317 (2022).
- [43] Q. J. Chen, Z. Q. Wang, R. Boyack, S. L. Yang, and K. Levin, When superconductivity crosses over: From BCS to BEC (2023), arXiv:2208.01774 [cond-mat.supr-con].
- [44] L. Liang, T. I. Vanhala, S. Peotta, T. Siro, A. Harju, and P. Törmä, Band geometry, Berry curvature, and superfluid weight, *Phys. Rev. B* **95**, 024515 (2017).
- [45] H. Guo, Y. He, C.-C. Chien, and K. Levin, Compressibility in strongly correlated superconductors and superfluids: From the BCS regime to Bose-Einstein condensates, *Phys. Rev. A* **88**, 043644 (2013).
- [46] X. Liu, Y. X. Chong, R. Sharma, and J. C. S. Davis, Discovery of a Cooper-pair density wave state in a transition-metal dichalcogenide, *Science* **372**, 1447 (2021).
- [47] L. F. Zhang, Y. M. Che, J. B. Wang, and Q. J. Chen, Exotic superfluidity and pairing phenomena in atomic Fermi gases in mixed dimensions, *Sci. Rep.* **7**, 12948 (2017).